

# Photon Flux and Wavelength Effects on the Selectivity and Product Yields of the Photocatalytic Air Oxidation of Neat Cyclohexane on TiO<sub>2</sub> Particles

Marta A. Brusa and Maria A. Grela\*

Departamento de Química, Facultad de Ciencias Exactas, Universidad Nacional de Mar del Plata, B7602AYL Mar del Plata, Buenos Aires, Argentina

Received: September 28, 2004; In Final Form: November 19, 2004

Product selectivity and yields of cyclohexanol and cyclohexanone formation in the photocatalytic air oxidation of cyclohexane on TiO<sub>2</sub> particles were determined as a function of the irradiation wavelength ( $254 \leq \lambda/\text{nm} \leq 366$ ) and the photon flux ( $0.3 \leq I_0/\text{neinstein cm}^{-2} \text{ s}^{-1} \leq 5.0$ ). Photonic efficiencies for total monoxygenated products (cyclohexanol + cyclohexanone) ranged from 10 to 25% depending on photon energy and fluency. The cyclohexanol-to-cyclohexanone ratio linearly increases with the incident photon flux at each wavelength and varies more than a magnitude order—from 3 to 32%—at the same incident photon fluency—5 neinstein  $\text{cm}^{-2} \text{ s}^{-1}$ —by changing the irradiation wavelength from 366 to 303 nm. Experimental evidence indicates that both spectral and intensity effects emerge as a consequence of the change in the frequency of photon absorption per particle. A mechanism is proposed which accounts for the origin of the selectivity changes.

## Introduction

Extensive work in the area of photoinduced electron-transfer processes at semiconductor interfaces is supported by the widespread of applications in relevant environmental processes such as photoelectrochemical solar cells and photocatalytic oxidation of air and water pollutants.<sup>1</sup> Also, the increasing awareness of the importance of conducting sustainable chemical process with minimal environmental impact has renewed the interest in the use of semiconductor photocatalysis for photosynthetic applications.<sup>2</sup> In this context, there is a great interest in the TiO<sub>2</sub>-photocatalyzed oxofunctionalization of hydrocarbons by molecular oxygen, which, under appropriate conditions can be carried with high selectivity and comparable efficiency to other methods.<sup>2,3</sup>

Particularly, it has early been reported that the photocatalytic oxidation of neat cyclohexane yields cyclohexanone as the main product and minor amounts of cyclohexanol (the selectivities are 83% and 5%, respectively). No other products except CO<sub>2</sub>, which evolves early in the reaction sequence, could be detected under typical reaction conditions.<sup>4,5</sup> It was also observed that the efficiency of monoxygenated products as well as product selectivity can be controlled by changing the solvent and/or by combining titanium dioxide with titanium silicate. For instance, Lu et al. found that UV irradiation of a system containing TiO<sub>2</sub> and titanium silicate dispersed in 50% mixtures of cyclohexane–acetonitrile changes the ratio between cyclohexanol and cyclohexanone and reduces the amount of CO<sub>2</sub> to less than 5%.<sup>6</sup>

More recently, Amadelli and co-workers investigated the effect of the solvent and oxygen on the photocatalytic oxidation of cyclohexane using TiO<sub>2</sub> powders dispersed in neat C<sub>6</sub>H<sub>12</sub> and C<sub>6</sub>H<sub>12</sub>/CH<sub>2</sub>Cl<sub>2</sub> mixtures. It was shown that an increase in the amount of dichloromethane brings about a decrease in CO<sub>2</sub> production and an enhancement in the rate of formation of cyclohexanone and cyclohexanol. Also, *R* increases from 0.05

to 0.5 on going from neat C<sub>6</sub>H<sub>12</sub> to 50% C<sub>6</sub>H<sub>12</sub>/CH<sub>2</sub>Cl<sub>2</sub> mixtures.<sup>7</sup> This behavior was addressed to a reduced adsorption of the intermediates on TiO<sub>2</sub> particles as the solvent becomes more polar. In fact, a recent study of Almquist et al. on cyclohexane photooxidation in different solvent mixtures showed that there is a strong correlation between cyclohexanol dark-adsorption isotherms and the predominance of the cyclohexanone among the monoxygenated products.<sup>8</sup>

We decided to reinvestigate this system to gain a better understanding of the origin of solvent effects on product distribution and total efficiency. However, we unexpectedly discovered that the yield of cyclohexanol in neat cyclohexane significantly depends on irradiation conditions.

In this paper, we report on the remarkable changes in product yields and selectivities in the TiO<sub>2</sub> photocatalytic oxidation of cyclohexane in pure liquid organic phase achieved by changing the incident photon flux and/or the irradiation wavelength under continuous wave irradiation. We provide experimental evidence in favor that both spectral and intensity effects emerge as a consequence of the associated changes in the frequency of photon absorption per particle, *Iap*.<sup>9–13</sup> The results herein presented may uncover a new perspective in the TiO<sub>2</sub>-photocatalyzed oxofunctionalization of hydrocarbons by molecular oxygen. Besides, on a pure academic basis they open new questions about the effects of photon intermittence.<sup>11,12,14</sup>

## Experimental Section

**Materials.** Degussa P25 was a commercial sample gently supplied by the manufacturers and used as provided. Cyclohexane (Cicarelli), cyclohexanone (Aldrich), cyclohexanol (Aldrich), and all other chemicals were of analytical reagent grade. Cyclohexane was further purified to remove traces of benzene following standard procedures and dried over CaCl<sub>2</sub>.<sup>15</sup>

**General Procedures.** Room temperature, air-saturated slurries (1 cm<sup>3</sup>, 2 g/L TiO<sub>2</sub>, [O<sub>2</sub>] = 2.3 mM) contained in square

\* Corresponding author. E-mail magrela@mdp.edu.ar.

prismatic silica cells (volume = 3 cm<sup>3</sup>) were fully illuminated with monochromatic radiation (from a Kratos-Schoeffel monochromator, 5 nm bandwidth) at several wavelengths. A magnetic stirring bar was used to ensure proper mixing and aeration during irradiation.

Photon flux determinations at each wavelength were performed by chemical actinometry using phenylglyoxylic acid as actinometer.<sup>16</sup> The incident photon flux,  $I_0$ , spanned the range  $3.6 \times 10^{-9} \leq I_0/\text{einstein cm}^{-2} \text{ s}^{-1} \leq 3.3 \times 10^{-10}$  at 303 nm,  $1.7 \times 10^{-9} \leq I_0/\text{einstein cm}^{-2} \text{ s}^{-1} \leq 1.0 \times 10^{-9}$  at 330 nm, and  $4.7 \times 10^{-9} \leq I_0/\text{einstein cm}^{-2} \text{ s}^{-1} \leq 5.1 \times 10^{-10}$  at 366 nm. These results were achieved by attenuating the direct photon emittance with fine mesh metal screens of different transmittance.

Product analysis were carried out by gas chromatography using a GLC system consisting of a Tracor 540 gas chromatograph, equipped with flame ionization (FID) and thermal conductivity (TCD) detectors. Intermediate products giving rise to GLC peaks were identified by comparing the retention time,  $t_r$ , with those of commercial standards. The concentrations of cyclohexanol and cyclohexanone were determined using the flame ionization detector (FID) and a 6' × 1/8" stainless steel, packed, 80/100, 10% DEGS, Chromosorb W column, with nitrogen as the carrier gas. Alternatively, the amount of cyclohexanone in some of the samples was also analyzed by HPLC. The HPLC system consisted of a gradient pump equipped with a UV-vis photodiode array detector (UV2000-Thermo Separation Products), equipped with a ODS, 5 μm, 250 mm × 4.6 mm, Phenomex column. Methanol/water 50 vol % was used as eluent, and the detection was performed at  $\lambda = 280$  nm. CO<sub>2</sub> concentration in the gas phase was determined by gas chromatography with a 6' × 1/8" stainless steel, packed, 100/120, Porapak R column, helium as carrier gas, and a thermal conductivity detector.

Initial photonic efficiencies for cyclohexanone,  $\xi_{\text{one}}$ , and cyclohexanol,  $\xi_{\text{ol}}$ , were calculated as the ratio between their initial generation rates and the incident photon flux,  $I_0$ .

## Results and Discussion

Gas chromatographic analysis of irradiated suspensions revealed only three products: cyclohexanone, cyclohexanol, and carbon dioxide. We verified that the amount of cyclohexanone determined by GLC was almost identical to that obtained by HPLC analysis. This check was undertaken because cyclohexyl hydroperoxide, a plausible intermediate in the early stages of cyclohexane oxidation,<sup>17</sup> readily decomposes upon GC injection into cyclohexanone and cyclohexanol in a ratio that depends on the chromatographic conditions (injector temperature, column type, etc.).<sup>18</sup> Additionally, total peroxides,  $P_T$ , were determined iodometrically following standard procedures.<sup>19</sup> By this way we established an upper limit,  $P_T < 50 \mu\text{M}$ , for the steady-state concentration of peroxides in the whole range of conditions investigated.

Figure 1 shows the accumulation of cyclohexanol and cyclohexanone during the course of a typical irradiation experiment. We observed that cyclohexanone-to-cyclohexanol ratio is nearly independent of the irradiation time within the range explored in the present work, typically between 1 and 4 mM of total products. Initial photonic efficiencies for cyclohexanone,  $\xi_{\text{one}}$ , and cyclohexanol,  $\xi_{\text{ol}}$ , formation were determined as a function of the photon flux and the irradiation wavelength. For comparison purposes, the photon dose in each irradiation experiment was adjusted in order to ensure nearly

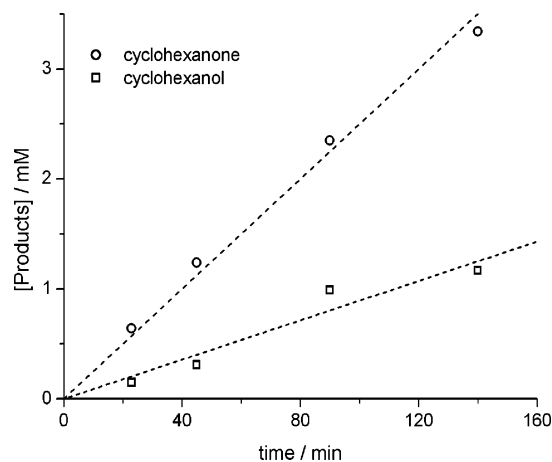


**Figure 1.** Yields of cyclohexanone (○) and cyclohexanol (□) as a function of the irradiation time.  $[\text{TiO}_2] = 2 \text{ g/L}$ ;  $I_0 = 3.64 \text{ neinstein cm}^{-2} \text{ s}^{-1}$ ;  $\lambda = 303 \pm 5 \text{ nm}$ .

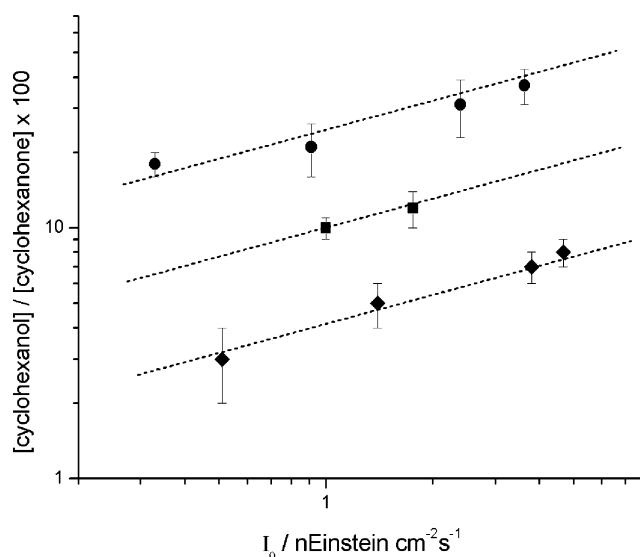


**Figure 2.** Ratio between cyclohexanol and cyclohexanone yields,  $R$ , vs the incident photon flux  $I_0$ , at various wavelengths,  $\lambda/\text{nm}$ : (●) 303, (■) 330, and (◆) 366. Bars show the typical dispersion obtained for at least five independent determinations.

the same yield of cyclohexanone, typically 1.5 mM, in all the determinations.

The most relevant data are presented in Figure 2 and indicate that  $R = \xi_{\text{ol}}/\xi_{\text{one}}$ <sup>20</sup> is a sensible function of the incident photon flux,  $I_0$ , and the irradiation wavelength,  $\lambda$ . It is worthwhile to say that the amount of CO<sub>2</sub> determined in these experiments did not display any appreciable trend with  $\lambda$  or  $I_0$  and nearly represent ~10–15% of total products ( $n(\text{CO}_2) = 0.18 \pm 0.04 \mu\text{mol}$ ). In all cases, mean values and standard deviations were obtained from at least five independent runs.

It is apparent from Figure 2 that the ratio between cyclohexanol and cyclohexanone splits into distinct sets at each wavelength but increases in a linear fashion with  $I_0$ . The fact that the data at each  $\lambda$  lies approximately on parallel lines guided us to consider that the spectral dependence may actually reflect the distinct frequency of photon absorption per particle through the dependence of the absorption coefficient,  $\alpha$ , with  $\lambda$ . Accordingly, we estimated the absorption coefficient at each wavelength as  $\alpha(\lambda) = 2.303A\rho/lc$ ,<sup>21</sup> where  $A$  is the absorbance of a 1.8 mM TiO<sub>2</sub> colloid sample recorded with an integrating sphere accessory (Hitachi U-3210 model, 60 mm sphere

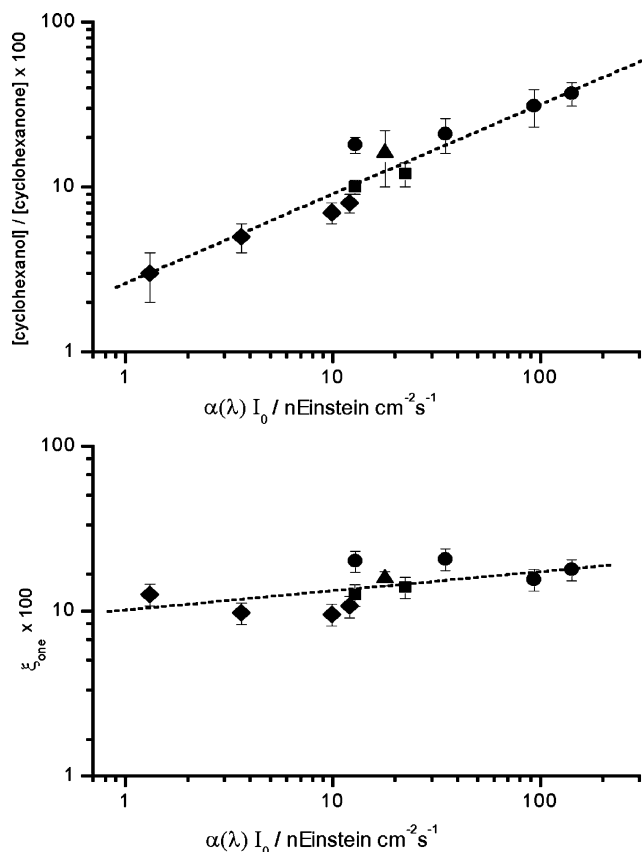
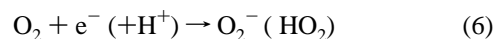
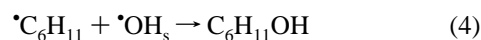
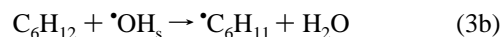
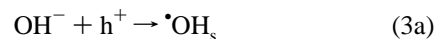
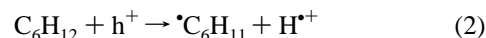
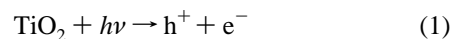


**Figure 3.** (a) Ratio between cyclohexanol and cyclohexanone yields,  $R$ , and (b) cyclohexanone initial photonic efficiency,  $\xi_{\text{one}}$ , vs  $\alpha(\lambda) \times I_0$ , at various wavelengths,  $\lambda$ : (▲) 254, (●) 303, (■) 330, and (◆) 366 nm. Bars show the typical dispersion obtained for at least five independent determinations.

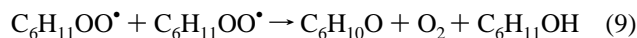
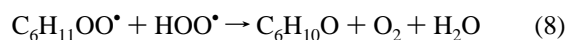
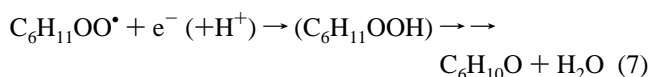
diameter, opening ratio 7.8%),  $l = 1$  cm is the path length,  $c$  is the  $\text{TiO}_2$  loading in the suspension, and  $\rho = 3.84 \text{ g cm}^{-3}$  is the density of the solid.<sup>22</sup> The resulting values at 254, 303, 330, and 366 nm were  $5.6 \times 10^4$ ,  $3.9 \times 10^4$ ,  $1.3 \times 10^4$ , and  $2.6 \times 10^3 \text{ cm}^{-1}$ , respectively. After evaluating the product  $\alpha(\lambda)I_0$ —a quantity proportional to  $Iap$ —we replotted the data using  $\alpha(\lambda)I_0$  as the abscissa. Figure 3a shows that all the experimental points are brought on a single line, indicating that the selectivity is mainly determined by photon intermittence and not by photon energy. Whatever the origins of the results presented in Figure 3, they appear to discard the strong adsorption of cyclohexanol and its rapid oxidation as the main reason for the low yields observed in previous investigations, which incidentally involve different irradiation conditions (i.e.,  $\lambda \geq 366$  nm).<sup>4,7,8</sup>

For completeness, the initial photonic efficiency for cyclohexanone formation is displayed in the bottom panel of Figure 3. Notice that  $\xi_{\text{one}}$  also correlates with  $Iap$ , although, considering the same frequency of photon absorption per particle, higher energy photons systematically appear to be somewhat more efficient.<sup>23</sup> Spectral dependencies on quantum yields have experimentally been observed in the polycrystalline  $\text{TiO}_2$ -photosensitized oxidations of some bifunctional aromatic compounds (chlorophenol,<sup>13,24</sup> salicylate,<sup>25</sup> nitrophenol,<sup>12</sup> and phthalate<sup>22</sup>), and different explanations have been put forward.<sup>13,22,26</sup> However, it is worthwhile to notice that product selectivity and quantum yields of the above-mentioned systems were found to be *independent* of the incident photon flux, at *variance* with present results.<sup>13b,22,25</sup>

In the following we intend to rationalize the unexpected experimental findings on the basis of the chemical nature of the possible involved intermediates shown in reactions 1–9.



Following the generation of the electron–hole pair by photon



absorption (reaction 1), the anodic process leads to  $\cdot\text{C}_6\text{H}_{11}$  radicals either by direct electron transfer (reaction 2) or through hole capture of adsorbed water molecules, followed by  $\text{HO}\cdot$  reaction with cyclohexane (steps 3a + 3b).<sup>27</sup>  $\text{O}_2$  addition to  $\cdot\text{C}_6\text{H}_{11}$  radicals proceeds under a diffusion-controlled rate in homogeneous solutions; therefore, we expected reaction 5 to be faster than reaction 4 under typical irradiation conditions. On the other hand, the high value of the C–H bond dissociation energy in cyclohexane renders H abstraction by  $\text{C}_6\text{H}_{11}\text{OO}\cdot$  species energetically unfavorable; thus, the fate of cyclohexylperoxy radicals will be determined by the competition between its reaction with the photogenerated electrons (reaction 7) and the bimolecular radical paths (8) and (9).<sup>28</sup> Considering that cyclohexyl hydroperoxide could not be detected in the course of our experiments, we assumed that it readily oxidizes to cyclohexanone.<sup>7,8</sup> In this context, it should be noticed that the thermal rearrangement of cyclohexyl hydroperoxide to cyclohexanone and water is a well-established intramolecular heterolytic reaction in acidic solutions.<sup>29</sup>

According to the simplified mechanism proposed for the initial stages of the reaction, the ratio cyclohexanol/cyclohexanone should be governed by the relative rates of reactions 4 + 9 to the overall processes that consume cyclohexylperoxy radicals, reactions 7–9. Although it is tempting to ascribe the selectivity changes to a progressive increment of the rate of reaction 4 with  $Iap$ ,<sup>9</sup> a closer analysis indicates that the competition between reactions 4 and 5 would require a similar number of  $\text{HO}\cdot$  radicals and  $\text{O}_2$  molecules in the vicinity of a nascent  $\cdot\text{C}_6\text{H}_{11}$  radical. This scenario is difficult to imagine, recalling that oxygen concentration in air-saturated cyclohexane solutions is  $[\text{O}_2]_s = 2.3 \text{ mM}$ .<sup>30</sup> Thus, we concluded that, to account for the results in Figure 3, the increment in the rate of photocarrier generation should be concomitant with an increment in the amount of cyclohexylperoxy radicals that disproportionate according reaction 9.<sup>31</sup> The above possibility can be rationalized

if the change in *Iap* portrays a modification in the relative rates of reactions 6 and 7, as discussed below.

Accordingly, we proposed that following electron–hole generation the anodic process readily leads to C<sub>6</sub>H<sub>11</sub>OO• (either through the sequence 2 + 5 or 3 + 5), and most of the photogenerated electrons become trapped before being scavenged through reaction 6 or 7.<sup>32</sup> Once in traps, electrons recombine or are removed from their surface states by C<sub>6</sub>H<sub>11</sub>OO• more readily than by O<sub>2</sub>, maintaining a different population of traps depending on *Iap*. Provided that only a *limited* number of surface states are available on any single particle, they may become saturated at moderate photon fluxes, and as a consequence, an increment in the rate of carrier generation will produce free conduction band electrons. This situation opens reaction 6 as an additional cathodic process and entails a progressive accumulation of cyclohexylperoxy radicals, since only a finite number of them are used to assist the renovation of the trap population. Thus, at low values of *I*<sub>0</sub> $\alpha$ , we propose that most of the generated C<sub>6</sub>H<sub>11</sub>OO• radicals react with trapped electrons, and almost all cyclohexanone comes from reaction 7. As *I*<sub>0</sub> $\alpha$  increases, the frequency of C<sub>6</sub>H<sub>11</sub>OO• generation rises, and the fraction of the organoperoxy radicals that is not reduced by the trapped electrons is channeled to reactions 8 and 9, providing a plausible, albeit tentative, explanation to the observed increase in the cyclohexanol/cyclohexanone ratio.

It should be noticed that the above argument requires reaction 7 to be slow enough to guarantee trap saturation at the relative moderate intensities used in this work. By assuming an average diameter of 30 nm for P25 TiO<sub>2</sub> particles, we estimated that the rates of photon generation per particle<sup>9</sup> are 10 and 1000 particle<sup>-1</sup> s<sup>-1</sup>,<sup>33</sup> at the limiting values of the abscissa in Figure 3 (*I*<sub>0</sub> $\alpha$  = 1 and 100 neinstein cm<sup>-2</sup> s<sup>-1</sup>, respectively). On the basis of these figures, electrons should persist trapped for more than 10 ms before being removed by reaction 7.<sup>33</sup> This represents a surprisingly high residence time for electrons in traps, even considering the difficulty of performing an electron-transfer reaction in a nonpolar media.<sup>34</sup> However, it is worthwhile to notice that a recent diffuse reflectance infrared spectroscopy study of illuminated dry TiO<sub>2</sub> powders indicates that electrons may survive for a few minutes in the presence of moist oxygen.<sup>11,35</sup>

The different reactivities of oxygen and cyclohexylperoxy radical toward trapped and free conduction band electrons may be accounted for on the basis of classical electron transfer theory. Accordingly, the rate constant for an interfacial electron-transfer process involving species A,  $k_{et} = \nu_n \kappa_{el} \kappa_n$ , is expressed in terms of a nuclear frequency parameter  $\nu_n$ , an electronic factor  $\kappa_{el}$ , and a nuclear factor  $\kappa_n$ .<sup>36</sup> The latter is given by eq 10, where  $\lambda$  is the reorganization energy and  $\Delta G^*$  stands for the driving force of the electron-transfer reaction.

$$\kappa_n = \exp\left[-\frac{(\Delta G^* + \lambda)^2}{4\lambda kT}\right] \quad (10)$$

For free carriers,  $\Delta G^*$  is the difference between the standard redox potential of the couple,  $E^\circ(A/A^-)$ , and the potential of the conduction band edge of the TiO<sub>2</sub> particle,  $E_{CB}(\text{TiO}_2)$ , while for trapped species  $\Delta G^* = E^\circ(A/A^-) - E_{CB}(\text{TiO}_2) - E_T$ , where  $E_T$  is the trap depth. Figure 4 represents a qualitative schematic energy diagram of the redox couples involved in reactions 6 and 7. For its construction we used, as reference, the band positions of aqueous TiO<sub>2</sub> suspensions at pH 7.0:  $E_{CB} = -0.32$  V and  $E_{VB} = 2.8$  V,<sup>37</sup> and the homogeneous redox potentials  $E^\circ(\text{C}_6\text{H}_{11}\text{OO}^\bullet/\text{C}_6\text{H}_{11}\text{OO}^-) = +0.8$  V<sup>38,39</sup> and  $E^\circ(\text{O}_2/\text{O}_2^\bullet-) = -0.16$  V<sup>40,41</sup> vs NHE. Although the actual values that apply to

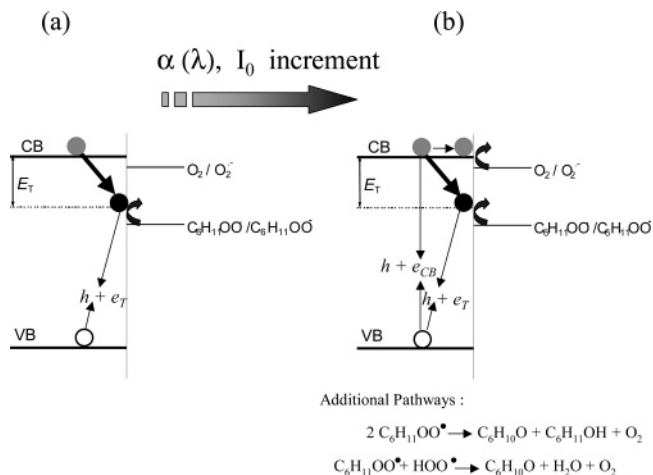


**Figure 4.** Qualitative energy diagram illustrating the proposed differences in the main reaction pathways at (a) low and (b) high values of the product  $\alpha(\lambda)I_0$ . Electron trapping is fast compared with the scavenging of conduction band electrons by O<sub>2</sub> or cyclohexylperoxy radicals, but limited by the number of surface states. Trapped electrons,  $e_T$ , recombine or are scavenged by cyclohexylperoxy radicals. Free conduction band electrons,  $e_{CB}$ , react with O<sub>2</sub>.

our system are expected to differ from those cited, we assumed that they nevertheless represent an approximate picture of the relative redox positions. It is apparent that  $\kappa_n$  for oxygen reduction by free electrons could be much higher than those corresponding to trapped species,<sup>12,42,43</sup> while the opposite will hold for the charge-transfer process involving cyclohexylperoxy radicals. Thus, we reasoned that the *relative* rate between reactions 6 and 7 is *reversed* by changing the nature of the carrier (free or trapped) that takes part in the charge-transfer event. It is recognized that the existence of a surface charge on TiO<sub>2</sub> particles may complicate the above analysis, since the electrochemical potential of the particle will naturally affect the rates of reactions 6 and 7. However, we assumed that charge buildup does not modify the conclusion that cyclohexylperoxy radicals cannot compete with O<sub>2</sub> for free conduction band electrons, and conversely O<sub>2</sub> reduction by trapped electrons is sluggish compared with the corresponding reduction of C<sub>6</sub>H<sub>11</sub>OO•.

An interesting point was raised by one of the referees, regarding whether our results could be influenced by the fact that Degussa P25 is actually a mixture of different crystalline phases (25% rutile–75% anatase). It is well-known that anatase shows an absorption spectrum that is blue-shifted from that of rutile due to the difference in their band gaps, 3.2 and 3.0 eV.<sup>44</sup> From Figure 1 of ref 44, we observed that the relative absorbances of pure anatase and rutile is  $\text{Abs}_{\text{anatase}}/\text{Abs}_{\text{rutile}} = 0.25$  at 366 nm and raises to 1 at  $\lambda \leq 350$  nm. Thus, by invoking different selectivities toward cyclohexanol of both crystalline phases, it would be possible to account for the observed differences in cyclohexanol/cyclohexanone ratio between 366 nm and the other wavelengths. However, by the same argument, *R* should remain constant at  $\lambda \leq 350$  nm and also be independent of *I*<sub>0</sub>, at variance with the results shown in Figures 2 and 3.

Summing up, although we cannot provide a definitive proof of the proposed mechanism, at least in theory, the behavior of this system may be explained on the basis of a limited number of surface states available for electron trapping which become saturated at relatively low absorption intensities and the fact that there exist two electron acceptors, oxygen and the organoperoxy radical, showing very different reactivities: the former

is added and the latter synthesized through a valence band process. Further work on these issues is currently underway.

## Conclusions

A quantitative photochemical study of the initial photocatalytic TiO<sub>2</sub> oxidation of cyclohexane reveals that product selectivity and total efficiency of monooxygenated products critically depend on the irradiation conditions. It becomes apparent that the frequency of photon absorption per particle rather than the photon energy is the main factor that controls the relative yield of cyclohexanol to cyclohexanone. A tentative explanation is given to rationalize the experimental findings based on the different reactivities of the two possible electron acceptors O<sub>2</sub> and C<sub>6</sub>H<sub>11</sub>OO• radicals toward trapped and free conduction band electrons.

**Acknowledgment.** This work was financially supported by the Agencia Nacional de Promoción de la Ciencia y la Tecnología de Argentina (ANPCyT), Project PICTO 06-11307. M.A.B. and M.A.G. are members of the National Research Council of Argentina (CONICET).

## References and Notes

- (1) Fox, M. A.; Dulay, M. T. *Chem. Rev.* **1993**, *93*, 341 and references therein.
- (2) Maldotti, A.; Molinari, A.; Amadelli, R. *Chem. Rev.* **2002**, *102*, 3811.
- (3) (a) Sun, H.; Blatter, F.; Frei, H. *J. Am. Chem. Soc.* **1996**, *118*, 6873. (b) Kiani, S.; Tapper, A.; Staples, R. J.; Stavropoulos, P. *J. Am. Chem. Soc.* **2000**, *122*, 7503. (c) Mizuno, N.; Nozaki, C.; Kiyoto, I.; Misono, M. *J. Am. Chem. Soc.* **1998**, *120*, 9267. (d) Raja, R.; Sankar, G.; Thomas, J. M. *J. Am. Chem. Soc.* **1999**, *121*, 11926.
- (4) Mu, W.; Herrmann, J. M.; Pichat, P. *Catal. Lett.* **1989**, *3*, 73.
- (5) Scalfani, A.; Herrmann, J. M. *J. Phys. Chem.* **1996**, *100*, 13655.
- (6) Lu, G.; Gao, H.; Suo, J.; Li, S. *J. Chem. Soc., Chem. Commun.* **1994**, 2423.
- (7) Boarini, P.; Carassiti, V.; Maldotti, A.; Amadelli, R. *Langmuir* **1998**, *14*, 2080.
- (8) Almquist, A. B.; Biswas, P. *Appl. Catal., A* **2001**, *214*, 259.
- (9) Müller, B. R.; Majoni, S.; Memming, R.; Meissner, D. *J. Phys. Chem. B* **1997**, *101*, 2501.
- (10) (a) Müller, M. L.; Borisch, J.; Raftery, D.; Francisco, J. S. *J. Am. Chem. Soc.* **1998**, *120*, 4537. (b) Xu, W.; Raftery, D.; Francisco, J. S. *J. Phys. Chem. B* **2003**, *107*, 4537.
- (11) (a) Cornu, C. J. G.; Colussi, A. J.; Hoffmann, M. R. *J. Phys. Chem. B* **2001**, *105*, 1351. (b) Cornu, C. J. G.; Colussi, A. J.; Hoffman, M. R. *J. Phys. Chem. B* **2003**, *107*, 3156.
- (12) Grela, M. A.; Colussi, A. J. *J. Phys. Chem. B* **1999**, *103*, 2614.
- (13) (a) Emeline, A.; Salinaro, A.; Serpone, N. *J. Phys. Chem. B* **2000**, *104*, 11202. (b) Emeline, A.; Serpone, N. *J. Phys. Chem. B* **2002**, *106*, 12221.
- (14) Wang, C. Y.; Pagel, R.; Bahnemann, D. W.; Dohrmann, J. K. *J. Phys. Chem. B* **2004**, *108*, 14082.
- (15) Perrin, D. D.; Armarego, W. L. F. *Purification of Laboratory Chemicals*; Pergamon Press: Oxford, 1988; p 131.
- (16) (a) Defoin, A.; Defoin-Straatmann, R.; Hildenbrand, K.; Bittersmann, E.; Krefit, D.; Kuhn, H. J. *J. Photochem.* **1986**, *33*, 237. (b) Kuhn, H. J.; Görner, H. *J. Phys. Chem.* **1988**, *92*, 6208.
- (17) Farkas, A.; Passaglia, E. *J. Am. Chem. Soc.* **1950**, *72*, 3333.
- (18) Shulpin, G. B.; Nizova, G. V. *React. Kinet. Catal. Lett.* **1992**, *48*, 333.
- (19) Furniss, B. S.; Hannaford, A. J.; Smith, P. W. S.; Tatchell, A. R. *Vogel's Textbook of Practical Organic Chemistry*; Addison Wesley Longman: Singapore, 1989; p 417.
- (20) Notice that possible errors in the absolute values of  $\xi_{ol}$  and  $\xi_{one}$  associated with some uncertainty in  $I_0$  determination is naturally canceled in  $R$ .
- (21) Serpone, N.; Lawless, D.; Khairutdinov, R. *J. Phys. Chem.* **1995**, *99*, 16646.
- (22) Grela, M. A.; Brusa, M. A.; Colussi, A. J. *J. Phys. Chem. B* **1999**, *103*, 6400.
- (23) A likely explanation is that higher values of  $\alpha$  entail a closer generation of the carriers to the semiconductor surface, probably reducing the rates of volume charge recombination.
- (24) Stafford, R.; Gray, K. A.; Kamat, P. V. *J. Catal.* **1997**, *167*, 25.
- (25) Grela, M. A.; Brusa, M. A.; Colussi, A. J. *J. Phys. Chem. B* **1997**, *101*, 10986.
- (26) Du, Y.; Rabani, J. *J. Phys. Chem. B* **2003**, *107*, 11970.
- (27) Gershuni, S.; Itzhak, N.; Rabani, J. *Langmuir* **1999**, *15*, 1141.
- (28) Goldstein, S.; Meyrestein, D. *Acc. Chem. Res.* **1999**, *32*, 547.
- (29) Deno, N. C.; Billups, W. E.; Kramer, K. E.; Lastomirsky, R. R. *J. Org. Chem.* **1970**, *35*, 3080.
- (30) Murov, S. L.; Carmichael, I.; Hug, G. L. *Handbook of Photochemistry*; Marcel Dekker: New York, 1993; p 290.
- (31) Carlsson, D. J.; Ingold, K. U. *J. Am. Chem. Soc.* **1968**, *90*, 1056.
- (32) Colombo, P. D., Jr.; Bowman, R. M. *J. Phys. Chem.* **1996**, *100*, 18445.
- (33) Recall that the required residence time of electrons in traps is tightened to the estimation of  $I_{ap}$ . In this context, it should be noticed that the nonpolar organic solvent favours TiO<sub>2</sub> particle aggregation. Thus, the half-life of trapped electrons may be lower than calculated since it is inversely correlated with photon intermittence.
- (34) Fox, M. A.; Ogawa, H. *J. Inf. Rec. Mater.* **1989**, *17*, 351.
- (35) Szczepankiewicz, S. H.; Colussi, A. J.; Hoffmann, M. R. *J. Phys. Chem. B* **2000**, *104*, 9842.
- (36) Grätzel, M. *Heterogeneous Photochemical Electron Transfer*; CRC Press: Boca Raton, FL, 1989.
- (37) Hoffmann, M. R.; Martin, S. T.; Choi, W.; Bahnemann, D. W. *Chem. Rev.* **1995**, *95*, 69.
- (38) Das, T. N.; Dhanasekaran, T.; Alfassi, Z. B.; Neta, P. *J. Phys. Chem. A* **1998**, *102*, 280.
- (39) Jonsson, M. *J. Phys. Chem.* **1996**, *100*, 6814.
- (40) Sawyer, D. T.; Valentini, J. S. *Acc. Chem. Res.* **1981**, *14*, 393.
- (41) Hoare, J. P. In *Standard Potentials in Aqueous Solution*; Bard, A. J., Parsons, R., Jordan, J., Eds.; Marcel Dekker: New York, 1987; Chapter 4.
- (42) Moser, J.; Punchedewa, S.; Infelta, P. P.; Grätzel, M. *Langmuir* **1991**, *7*, 3012.
- (43) Gerischer, H.; Heller, A. *J. Electrochem. Soc.* **1992**, *139*, 113.
- (44) Torimoto, T.; Nakamura, N.; Ikeda, S.; Ohtani, B. *Phys. Chem. Chem. Phys.* **2002**, *4*, 5910.